-RESEARCH PAPER-

International Journal of Mining and Geo-Engineering

IJMGE

IJMGE 59-1 (2025) 69-74

DOI: 10.22059/IJMGE.2025.383290.595200

Enhancing core recovery and RQD analysis in porphyry Cu deposits through fractal modelling, case study: Sungun mine (NW Iran)

Peyman Afzal [a, b] *, Behzad Heidari [a], Mohsen Alidaryan [a], Behnam Sadeghi [c, d] and Lili Daneshvar Saein [e]

[a] Pouya Mes Iranian Company, Tehran, Iran.

[b] Department of Petroleum and Mining Engineering, Islamic Azad University, Tehran, Iran.

[c] Earth and Sustainability Science Research Centre, School of Biological, Earth and Environmental Sciences, University of New South Wales, NSW 2052, Australia.

[d] CSIRO Mineral Resources, Australian Resources Research Centre, Kensington, WA 6151, Australia.

[e] Department of Geology, Payame Noor University, PO Box19395-3697, Tehran, Iran.

Article History:

Received: 12 October 2024.
Revised: 24 December 2024.
Accepted: 12 February 2025.

ABSTRACT

Interpreting core samples is a critical task in mineral exploration, essential for mine planning and design. Core Recovery (CR) and Rock Quality Designation (RQD) are key factors in assessing the geomechanical properties of a deposit during coring operations. This is particularly important in porphyry deposits, which are notable for hosting significant, deep copper mines. The accurate determination and interpretation of core recovery and RQD are crucial for these porphyry deposits. This study applied number-size (N-S) fractal modelling to enhance the interpretation of core recovery and RQD in ongoing exploratory drilling at the Sungun porphyry deposit, a prominent copper mine in Iran. Our findings revealed that core recovery and RQD exhibited a multifractal nature. Key zones for core recovery and RQD began at thresholds of 75% and 63%, respectively, with high-intensity zones for both parameters started at 89%. Additionally, the study explored correlations between these zones and other drilling parameters, such as mud flush return, drilling time, and core length, using an overall accuracy (OA) matrix. These parameters were analyzed using the N-S fractal model, indicated a strong relationship between core recovery, core length, flush returns, and drilling time. This integrative approach enhances our understanding of the deposit's geomechanical properties and guides more effective exploration strategies.

Keywords: *Core Recovery (CR), Rock Quality Designation (RQD), Number-Size (N-S) fractal modelling, Porphyry, Sungun.*

1. Introduction

Core drilling is a crucial procedure in the detailed and supplementary exploration phases across various mineral deposits. This operation yields valuable parameters, notably the Core Recovery (CR) and Rock Quality Designation (RQD), which are vital for the geomechanical interpretation and the accuracy of exploratory data [1]. These parameters are instrumental in optimizing core drilling operations, calculating bit penetration rates, and facilitating resource/reserve evaluation and mine design/planning [2-5]. Moreover, the RQD is an essential metric for determining the Rock Mass Rating (RMR) across various mining environments [5-7]. These metrics gain added significance in magmatic/hydrothermal ore deposits, particularly porphyry deposits, which are major sources of copper, molybdenum, and gold. Porphyry deposits also host some of the world's largest and deepest open-pit mines, such as Escondida, Chuquicamata, Bingham Canyon, Grasberg, Sarcheshmeh, and Sungun. The host rocks of these deposits are typically sub-volcanic and plutonic massive units, including granodiorite, quartz-diorite, monzodiorite, monzogranite, and quartz-monzonite, noted for their high hardness values [8-10]. Core recovery is also crucial for the geochemical analysis of core samples, and samples with a CR lower than 75% are generally considered unsuitable for chemical analysis.

Statistical, geostatistical, and fractal methodologies have been extensively applied in describing geological features and phenomena, particularly in mining-related fields. These approaches are instrumental in understanding lithological units, alteration zones, ore grades, geomechanical characteristics, and the RQD analysis [11-14]. Introduced by [35], fractal geometry, a principal nonlinear geometry, has been widely adopted in geological sciences and mining engineering ([15-18]; [19-22]). This has led to the development of various multifractal models for geotechnical, geophysical, petrophysical, and geochemical modelling to define different zones ([19], [23-27], [41]).

For example, Yasrebi et al. [4] employed the RQD-Number (RQD-N) and RQD-Volume (RQD-V) methods at the Kahang porphyry deposit in Central Iran to aid in rock mass characterization. Additionally, [12] utilized multivariate fractal modelling to delineate geomechanical zones in the Chadormalu iron open pit mine, demonstrating the effectiveness of these advanced mathematical techniques in practical mining applications. The purpose of this procedure was to enhance the use of fractal modelling for CR and RQD to improve the interpretations of core drilling operations at the Sungun Cu porphyry deposit, a world-class open-pit mine in Iran. We specifically employed the RQD-N and Core Recovery-Number (CR-N)

* Corresponding author. *E-mail address:* peymanafzal@yahoo.com (P. Afzal).

multifractal models to differentiate various rock mass zones obtained by coring data via the Sungun deposit. Subsequently, the outcomes derived from these fractal models were cross-referenced and validated by associated drilling parameters, such as mud flush return, drilling time, and core length, which were analyzed using an overall accuracy (OA) matrix (see [40]). This integrative approach seeks to establish a robust framework for assessing drilling efficiency and geological consistency in complex ore deposits.

2. Materials and methodology

2.1. Case study

The Miocene Sungun Cu-Mo porphyry is situated to the northwest of the Urumieh-Dokhtar magmatic belt in Northwestern Iran, a key geological feature depicted in various studies (Fig. 1). This region is significant as it sits along the suture zone between Eurasian and Afro-Arabian plates, where the subduction of the Neo-Tethys oceanic plate has led to the formation of major Iranian porphyry deposits [28-31].

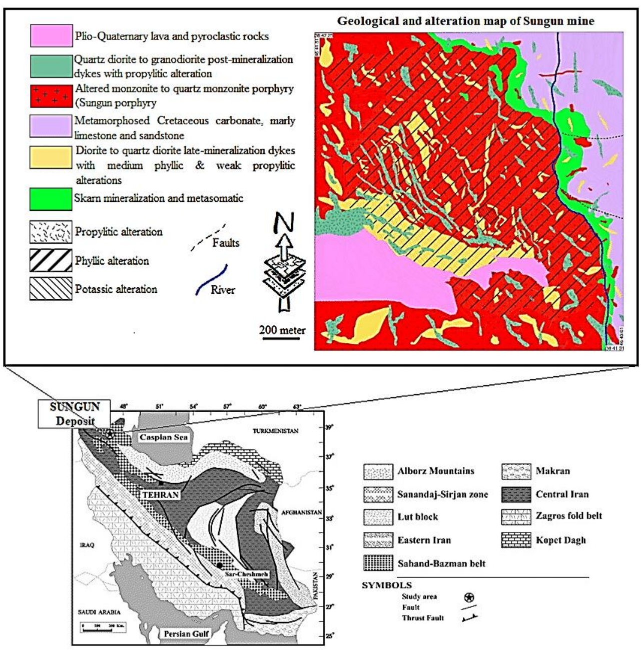

(a)

Fig. 1. a) Location and geological map of the Sungun copper porphyry deposit [34], and b) a core of mineralized zone from Sungun mine.

The earliest intrusive activity in this area is represented by a quartz-monzonite pluton, which serves as the primary host for the porphyry Cu-Mo ores found in the region [32]. The Sungun mine itself encompasses the mineral-rich Sungun porphyry along with six groups of post-mineralization dykes that are both cross-cutting and lithologically distinct. These dykes, which display a NW-SE orientation and SW dip, vary in composition, including quartz diorite, gabbro, diorite, dacite, lamprophyre, and microdiorite [32].

Additionally, the mine features extensive alteration zones, such as propylitic, argillic, phyllic, and potassic zones, which play a crucial role in the geology of the mine and its potential for mineral extraction. These alteration zones are key indicators of the hydrothermal processes that have significantly influenced the mineralogy and economic potential of the Sungun deposit.

The oldest geological formations in this deposit consist of the 500-meter sequence of Cretaceous limestone, which is interspersed with layers of shale. This stratigraphy is crucial for understanding the sedimentary history and potential mineral content of the region. During ongoing exploration and exploitation activities, the estimated reserves and resources have shown significant increases, reaching over 850 million tons and 5 billion tons, respectively [33]. This substantial growth in estimated reserves and resources highlights the economic and geological potential of the area, suggesting a rich deposit that could be vital for future mining endeavors.

2.2. Dataset

The coring data collected from the Sungun mine comprised 13,382 core samples obtained from 27 drilled boreholes using four different drilling machines (Fig. 2). This extensive dataset included valuable parameters, such as CR, RQD, the length of the cores, the time of drilling, and the flush return of mud drilling. These boreholes were drilled as part of a new exploration initiative at the Sungun mine during the years 2022 and 2023.

Importantly, the coring data were extracted from the mineralized zones of the Sungun porphyry and also from a porphyry stock. This dual source of samples enriched the dataset, providing a comprehensive view of the geological and mineralogical variability within the mine. The data thus not only enhances our understanding of the existing mineral resources but also aids in the effective planning and execution of subsequent mining and exploration activities.

Fig. 2. Several exploratory cores from drilling operation in the Sungun mine.

2.3. N-S model

The N-S modelling is described by this following equation [35]; also see [15]; [36]; [38-39]:

$$N(\geqslant \rho) = F\rho^{-D} \tag{1}$$

The ρ shows CR and RQD values; $N(\geq \rho)$ indicates samples' cumulative number for RQD or CR values equal or more than to ρ; F and D are a constant and the scaling exponent/fractal dimension for distribution of RQD values. According to [35], log–log plots based on $N(\geq\rho)$ against ρ depict straight line segments with various slopes $-D$ corresponding to different RQD or CR break points.

2.4. Overall Accuracy (OA) matrix

The OA matrix [40], is a 2x2 matrix designed to calculate the overlapping among two binary models/datasets. This matrix is particularly useful in assessing the correlation and consistency between classes derived through fractal modelling of the CR and RQD, as depicted in Table 1.

In practical terms, the OA matrix compares predicted outcomes to actual values, helping to quantify the degree of agreement between two datasets. The matrix setup typically involves two categories or classes from each model, with the matrix entries reflecting counts of data points falling into each combination of predicted and actual categories.

If the OA value exceeds 0.5, this indicates a satisfactory level of overlap, meaning that the two datasets or models have a substantial agreement or consistency in the classifications they provide. This measure is critical when evaluating the effectiveness of fractal models in geotechnical analysis, allowing researchers and engineers to verify the reliability of interpretations made from core sample data. The application of the OA matrix in this context supports more informed decision-making in mining exploration and development activities [37].

3. Results and Discussion

3.1. Application of fractal modelling

The N-S fractal modelling applied to the CR and RQD data delineated four and five zones respectively, as indicated in the related log-log plots (Fig. 3). This demonstrated the multifractal nature of both parameters, also illustrated in Fig. 3. The major zones for the CR and RQD commenced at thresholds of 75% and 63%, respectively. Additionally, the threshold for high-intensity zones for both parameters was consistent, started at 89%. Conversely, zones categorized as low quality for the CR and RQD were identified below 45% and 12%, respectively.

Furthermore, the N-S fractal modelling was applied to additional drilling parameters, such as flush return of mud drilling, time of drilling, and length of cores, as depicted in Fig. 4. The flush return exhibited bifractal behavior with a key threshold at 76%. The length of cores was differentiated by three thresholds: 0.5, 0.9, and 2 meters, with lengths ≥ 2 meters constituted the main zone for this parameter. The log-log plot for the time of coring operation revealed three thresholds at 32, 80, and 158 minutes. Notably, times shorter than 80 minutes were identified as the major zone for drilling operations and were associated with the higher values of CR and RQD. Consequently, the primary zones for flush return of mud drilling, time of drilling, and length of cores were established at ≥76%, ≤80 minutes, and ≥2 meters, respectively.

3.2. Application of OA matrix

The N-S model findings revealed significant correlations between the main zones for the CR and RQD, as well as the major operational parameters, including time, length, and flush return of mud drilling (Tables 2 to 9). Specifically, the correlation between high-intensity zones where both the CR and RQD were ≥89% was approximately 61%, as detailed in Table 2. Moreover, the major zones where CR values were ≥75% and RQD values were ≥63% exhibited a correlation of about 79%, as depicted in Table 3. These correlations underscored a direct relationship between CR and RQD, indicated that higher recovery and rock quality were consistently associated with the drilling cores from the Sungun mine.

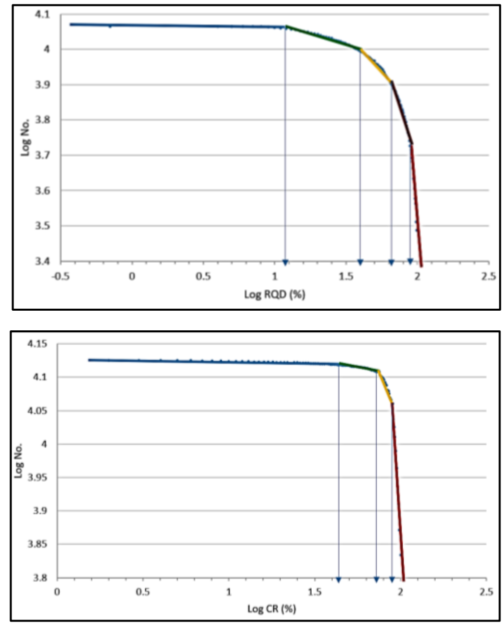

Fig. 3. CR-N and RQD-N log-log plots for the Sungun mine drilling data.

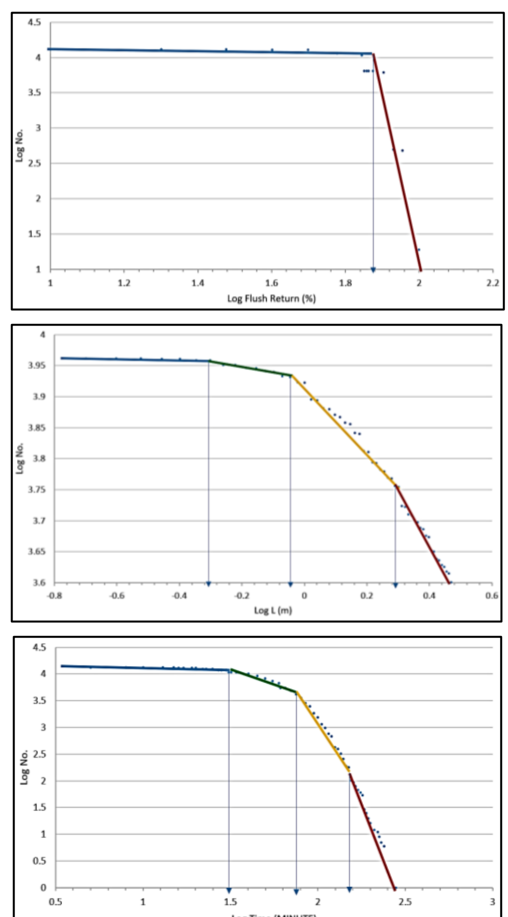

Fig. 4. The N-S log-log plots for time, length, and flush return in the Sungun mine drilling data.

Futhermore, high-intensity CR zones with values ≥89% were compared with a flush return of ≥76%, as presented in Table 4. The OA of this comparison was approximately 61%, indicated a proper correlation between these parameters. Furthermore, the OA between the high-intensity zone for CR and the length of cores, with respective thresholds of ≥89% and ≥2 meters, was 62%. Moreover, the correlation between the high-intensity CR zone and coring times of ≤80 minutes showed a robust OA of about 80%, as noted in Table 6. These comparisons demonstrated a direct correlation between CR and both the length of cores and the flush return of mud drilling. Conversely, there was a reverse relationship between CR and the timing of the coring operation, suggesting that faster drilling times may correspond to higher core recovery rates. High-intensity RQD zones (≥89%) were compared with the main zones of flush return of mud drilling, time of drilling, and length of cores. The comparison revealed a less than optimal OA of 48% between the high-intensity RQD zone and the main timing of coring (≤ 80 minutes), as shown in Table 7. This lower OA suggested that other factors, such as the experience of the operator and the quality of the drilling rig, might significantly influence the results.

Conversely, there was a strong correlation between the high-intensity RQD zone and the main zone of core length, with an OA of 80%, indicated a good relationship, as detailed in Table 8. Also, a direct relationship was observed between the high-intensity RQD zone and the main zone of flush return of mud drilling, with an OA of about 57%, as depicted in Table 9. These findings highlight varying degrees of correlation between RQD and different drilling parameters.

Table 1. OA Matrix for Comparing Fractal Modelling Results of the CR and RQD.

		CR fractal model	
		Inside zone	Outside zone
RQD fractal model	Inside zone	True positive (A)	False positive (B)
	Outside zone	False negative (C)	True Negative (D)
		Type I error=C/(A+C)	Type II error=B/(B+D)
		OA=(A+D)/(A+B+C+D)	

Table 2. OA Matrix for Comparing of High Intensity Zones for the CR and RQD.

		CR≥89%	
		Inside zone	Outside zone
RQD≥89%	Inside zone	4529	6958
	Outside zone	2	6422
		Type I error=0.0004	Type II error=0.52
		OA= 0.61	

Table 3. OA Matrix for Comparing Performance of Major Zones for the CR and RQD.

		CR≥75%	
		Inside zone	Outside zone
RQD≥63%	Inside zone	8233	4585
	Outside zone	5	8795
		Type I error=0.0006	Type II error=0.34
		OA= 0.79	

Table 6. OA Matrix for Comparing Performance of High Intensity Zones for the CR and Timing of Coring.

		Timing of coring≤ 80 minutes	
		Inside zone	Outside zone
CR≥89%	Inside zone	8833	2654
	Outside zone	1714	9014
		Type I error=0.16	Type II error=0.99
		OA= 0.803	

Table 7. OA Matrix for Comparing Performance of High Intensity Zones for the RQD and Timing of Coring.

		Timing of coring≤ 80 minutes	
		Inside zone	Outside zone
CR≥89%	Inside zone	3525	1813
	Outside zone	7022	4547
		Type I error=0.66	Type II error=0.28
		OA= 0.48	

Table 8. OA Matrix for Comparing Performance of High Intensity Zones for the RQD and Length of Cores.

		Length of cores≥ 2 m	
		Inside zone	Outside zone
RQD≥89%	Inside zone	4425	913
	Outside zone	2708	9761
		Type I error=0.38	Type II error=0.085
		OA= 0.80	

Table 9. OA Matrix for Comparing Performance of High Intensity Zones for the RQD and Flush Return of Mud Drilling.

		Flush return≥76%	
		Inside zone	Outside zone
RQD≥89%	Inside zone	2362	2975
	Outside zone	3811	6596
		Type I error=0.62	Type II error=0.31
		OA= 0.57	

4. Conclusions

The findings from this study highlighted a direct correlation between CR and RQD in the Sungun copper mine. This relationship likely arose from geological specifics, particularly related to drilling within the Sungun porphyry. Additionally, CR showed a robust positive correlation with the flush return of mud drilling, the duration of drilling, and the length of cores.

Moreover, positive relationships existed between RQD and both the length of cores and the flush return of mud drilling. However, the correlation between RQD and the timing of coring was moderate, falling below 50%. This lesser correlation may be attributed to factors, such as the experience of the drilling operator and the capability of the drilling equipment. Additionally, geological features, such as faults and fractures may also significantly influence this outcome. Deep core drilling is an important and general operation for porphyry deposits exploration, such as Sungun deposit. This methodology can be used for better designing of core drilling grid and drilling project for optimization of core drilling operation, e.g., increasing of velocity, CR, RQD and also better geochemical analysis.

Acknowledgements

The authors would like to express their gratitude to Pouya Mes Iranian Exploration Engineering Company for their support of this research, particularly in providing the dataset.

References

[1] Zhang, L., 2016. Determination and applications of rock quality designation (RQD). Journal of Rock Mechanics and Geotechnical Engineering 8(3), 389-397.

[2] Hustrolid W., Kuchta M., 2006. Open Pit Mine Planning and Design (2th Edition). 972 p.

[3] Aalizad, S.A., Rashidinejad, F., 2012. Predication of Peneteration Rate of Rotary-Percussive Drilling Using Artificaial Neural Networks – A Case Study. Arch. Min. Sci. 57 (3), 715–728.

[4] Yasrebi, A.B., Wetherelt, A., Foster, P.J., Afzal, P., Coggan, J., Ahangaran, D.K., 2013. Application of RQD-Number and RQD-Volume multifractal modelling to delineate rock mass characterisation in Kahang Cu-Mo porphyry deposit, central Iran. Archives of Mining Sciences 58 (4), 1023-1035.

[5] Chen, Q., Yin, T., Niu, W. 2018. Replacing RQD and Discontinuity Spacing with the Modified Blockiness Index In the Rock Mass Rating System. Arch. Min. Sci. 63 (2), 353-382.

[6] Hasan, M., Shang, Y., Yi, X., Shao, P., He, M., 2023. Determination of rock mass integrity coefficient using a non-invasive geophysical approach. Journal of Rock Mechanics and Geotechnical Engineering 15(6), 1426-1440.

[7] Hasan, M., Shang, Y., Meng, Q., 2023. Evaluation of rock mass units using a non-invasive geophysical approach. Scientific Reports 13, 14493.

[8] Pirajno, F., 2009. Hydrothermal Processes and Mineral Systems. Springer, 1250 p.

[9] Daneshvar Saein, L., 2017. Delineation of enriched zones of Mo, Cu and Re by concentration-volume fractal model in Nowchun Mo-Cu porphyry deposit, SE Iran. Iranian Journal of Earth Sciences 2, 64-72.

[10] Aghazadeh, M., Hou, Z., Badrzadeh, Z., & Zhou, L., 2015. Temporal spatial distribution and tectonic setting of porphyry copper deposits in Iran: Constraints from zircon U-Pb and molybdenite Re–Os geochronology. Ore Geology Reviews 70, 385–406.

[11] Yasrebi, A.B., Wetherelt, A., Foster, P., Coggan, J., Afzal, P., Agterberg, F., Kaveh Ahangaran, D., 2014. Application of a density–volume fractal model for rock characterisation of the Kahang porphyry deposit. International Journal of Rock Mechanics and Mining Sciences 66, 188-193.

[12] Mahdizadeh, M., Afzal, P., Eftekhari, M., Ahangari, K., 2022. Geomechanical zonation using multivariate fractal modeling in Chadormalu iron mine, Central Iran. Bulletin of Engineering Geology and the Environment 81 (1), 59

[13] Malaekeh, A., Ghassemi, M.R., Afzal, P., Solgi, A., 2021. Fractal modeling and relationship between thrust faults and carbonate-hosted Pb-Zn mineralization in Alborz Mountains, Northern Iran. Geochemistry 81 (4), 125803.

[14] -Monjezi, M., Baghestani, M., Afzal, P., Yarahmadi Bafghi, A.R., Hashemi, S.A., 2024. Investigation on Relationship between Rock Characteristics and Blasting Fragmentation using Fractal Analysis. Journal of Mining and Environment 10.22044/jme.2024.15240.2917

[15] Agterberg F.P., 1995. Multifractal modeling of the sizes and grades of giant and supergiant deposits. International Geology Review 37, 1–8.

[16] Cheng, Q., 1999. Multifractality and spatial statistics. Comput. Geosci. 25, 949-961.

[17] Cheng, Q., Agterberg, F.P., Ballantyne S.B., 1994. The separation of geochemical anomalies from background by fractal methods. Journal of Geochemical Exploration 51, 109-130.

[18] Li, C., Ma, T., Shi, J., 2003. Application of a fractal method relating concentrations and distances for separation of geochemical anomalies from background. Journal of Geochemical Exploration 77, 167-175.

[19] Afzal, P., Alghalandis, Y.F., Khakzad, A., Moarefvand, P., Rashidnejad Omran, N., 2011. Delineation of mineralization zones in porphyry Cu deposits by fractal concentration–volume modeling. Journal of Geochemical exploration 108 (3), 220-232

[20] Afzal, P., Alghalandis, Y.F., Moarefvand, P., Rashidnejad Omran, N., Asadi Haroni, H., 2012. Application of power-spectrum–volume fractal method for detecting hypogene, supergene enrichment, leached and barren zones in Kahang Cu porphyry deposit, Central Iran. Journal of Geochemical Exploration 112, 131-138.

[21] Ghosh, A., Daemen J.J., Van Zyl D., 1990. Fractal-based approach to determine the effect of discontinuities on blast fragmentation. In: The 31th US Symposium on Rock Mechanics (USRMS), American Rock Mechanics Association.

[22] Pourgholam, M.M., Afzal, P., Adib, A., Rahbar, K., Gholinejad M., 2024. Recognition of REEs anomalies using an image Fusion fractal-wavelet model in Tarom metallogenic zone, NW Iran. Geochemistry, 126093.

[23] Afzal, P., Abdideh, M., Daneshvar Saein, L., 2023. Separation of productivity index zones using fractal models to identify promising areas of fractured reservoir rocks. Journal of Petroleum Exploration and Production Technology 13 (9), 1901-1910.

[24] Crum, S.V., 1990. Fractal concepts applied to bench-blast fragmentation. In: Proc. 3rd US Rock Mech. Symp. Balkema, Rotterdam 913–919..

[25] Daneshvar Saein, L., Afzal, P., 2017. Correlation between Mo mineralization and faults using geostatistical and fractal modeling in porphyry deposits of Kerman Magmatic Belt, SE Iran. Journal of Geochemical Exploration 181, 333-343.

[26] Koohzadi, F., Afzal, P., Jahani, D., Pourkermani, M., 2021. Geochemical exploration for Li in regional scale utilizing Staged Factor Analysis (SFA) and Spectrum-Area (SA) fractal model in north central Iran. Iranian Journal of Earth Sciences 13 (4), 299-307.

[27] Sadeghi, B., 2024. Fractals and Multifractals in the Geosciences. Elsevier, Amsterdam (https://doi.org/10.1016/B978-0-323-90897-9.00010-9).

[28] Aghazadeh, M.; Hou, Z.; Badrzadeh, Z.; Zhou, L. Temporal–spatial distribution and tectonic setting of porphyry copper deposits in Iran: Constraints from zircon U–Pb and molybdenite Re–Os geochronology. Ore Geol. Rev. 2015, 70, 385–406.

[29] Zürcher, L.; Bookstrom, A.A.; Hammarstrom, J.M.; Mars, J.C.; Ludington, S.; Zientek, M.L.; Dunlap, P.; Wallis, J.C.; Drew, L.J.; Sutphin, D.M.; et al. Porphyry Copper Assessment of the Tethys Region of Western and Southern Asia: Chapter V in Global Mineral Resource Assessment; US Geological Survey: Reston, VA, USA, 2015.

[30] Richards, J.P.; Sholeh, A. 2016. The Tethyan tectonic history and Cu-Au metallogeny of Iran. Econ. Geol. Spec. Publ. 19, 193–212.

[31] Ehlen, J., 2000. Fractal analysis of joint patterns in grantie. Int J Rock Mech Min Sci 37(6), 909–922.

[32] Kamali, A.A., Moayyed, M., Amel, N., Hosseinzadeh, M.R., Mohammadiha, K., Santos, J.F., Brenna, M. 2018. Post-Mineralization, Cogenetic Magmatism at the Sungun Cu-Mo Porphyry Deposit (Northwest Iran): Protracted Melting and Extraction in an Arc System. Minerals, 8(12), 588.

[33] Kou, G.Y., Xu, B., Zhou, Y., Zheng, Y.C., Hou, Z.Q., Zhou, L.M., Zhang, Y.F., Yu, J.X. 2021. Geology and petrogenesis of the Sungun deposits: Implications for the genesis of porphyry-type mineralisation in the NW Urumieh–Dokhtar magmatic Arc, Iran. Ore Geology Reviews 131, 104013.

[34] Talesh Hosseini, S., O. Asghari, Torabi, S.A., Abedi, M. 2020. An Optimum Selection of Simulated Geological Models by Multi-Point Geostatistics and Multi-Criteria Decision-Making Approaches; a Case Study in Sungun Porphyry-Cu deposit, Iran. Journal of Mining and Environment 11(2), 481-503.

[35] Mandelbrot B.B., 1983. The Fractal Geometry of Nature. W.H. Freeman, San Francisco, CA. Updated and Augmented Edition.

[36] Ahmadi, N.R., Afzal, P., Yasrebi, A.B., 2021. Delineation of gas content zones using NS fractal model in coking coal deposits. Journal of Mining and Environment 12 (1), 181-189

[37] Ficker, T., 2017. Fractal properties of joint roughness coefficients. Int J Rock Mech Min Sci 94, 27–31.

[38] Sadeghi, B., 2021. Simulated-multifractal models: a futuristic review of multifractal modeling in geochemical anomaly classification. Ore Geology Reviews, 139 (Part B) (https://doi.org/10.1016/j.oregeorev.2021.104511).

[39] Hassanpour, S., Afzal, P., 2013. Application of concentration–number (C–N) multifractal modeling for geochemical anomaly separation in Haftcheshmeh porphyry system, NW Iran. Arabian Journal of Geosciences 6, 957-970

[40] Carranza, E.J.M., 2011. Analysis and mapping of geochemical anomalies using logratio-transformed stream sediment data with censored values. Journal of Geochemical Exploration 110: 167-185.

[41] Nikzad, M.R., Asadi, A., Kaveh Ahangaran, D., Yasrebi, A.B. Wetherelt, A., Afzal, P., 2018. Application of fractal modelling to classify blast fragmentation and size distributions. Archives Mining of Sciences 63(3), 783-796.